Diffraction pattern calculations for a certain class of *N*-fold quasilattices

1998 J. Phys. A: Math. Gen. 31 6873

(http://iopscience.iop.org/0305-4470/31/32/011)

J. Phys. A: Math. Gen. **31** (1998) 6873–6886. Printed in the UK PII: S0305-4470(98)90619-9

Diffraction pattern calculations for a certain class of N-fold quasilattices

Przemyslaw Repetowicz†§ and Janusz Wolny‡
† Institut für Physik, Technische Universität Chemnitz, D-09107 Chemnitz, Germany
‡ Faculty of Physics and Nuclear Techniques, University of Mining and Metallurgy al. Mickiewicza 30, 30-059 Cracow, Poland

Received 12 January 1998, in final form 30 April 1998

Abstract. Using the 'cut-and-project' method we obtain seven- and nine-fold quasiperiodic lattices. For such quasilattices the structure factors are calculated analytically through integration in higher-dimensional spaces. The obtained formulae are compared with the direct numerical calculations of Fourier transforms.

1. Introduction

The goal of this paper is to carry out analytical calculations of the diffraction pattern of a certain class of N-fold quasilattices which can be generated by a projection from a higher-dimensional space [1]. Whereas the case of $N \leqslant 5$ has been already examined many times before [7] the generic case of $N > 5$ does not seem to have been tackled. Several papers [2] have been scarcely devoted to some scaling properties of the regarded diffraction patterns, in relation to the self-similarity of quasilattices, which can be analysed without performing analytical calculations of the structure factor. We would like to show that the mathematical difficulties encountered by the extension of the calculation formalism from the case $N = 5$ to the generic one can be easily solved.

2. An N-fold quasilattice and its diffraction pattern

We consider a class of N-fold quasilattices, where N is odd. These quasilattices can be generated by the cut-and-project method [1, 7] from the N-dimensional space (see figures 1 and 2 for representatives of seven- and nine-fold quasilattices respectively). The quasilattices can also be regarded as tilings built from $\frac{N-1}{2}$ kinds of unit rhombuses with angles $\frac{2\pi}{N}$, $\frac{2\cdot 2\pi}{N}, \ldots, \frac{2\cdot(N-1)\pi}{2\cdot N}$ respectively. With respect to the way of generation they are similar to the Penrose quasilattice, because both the orientation of the projection plane E, embedded in the N-dimensional space, and the choice of the projection strip obey the same rules as for the Penrose quasilattice. The projection plane E is chosen as an invariant subspace with respect to a following permutation g of the unit vectors $\boldsymbol{e}_i$ of the N-dimensional space: $\mathrm{g}(\boldsymbol{e}_i) = \boldsymbol{e}_{i+1}$. More precisely, the vectors spanning E read:

$$\boldsymbol{v}_0 = (v_{0j})_{j=1}^N = \sqrt{\frac{2}{N}}\left(\cos\frac{2\pi j}{N}\right)_{j=1}^N \qquad \text{and} \qquad \boldsymbol{w}_0 = (w_{0j})_{j=1}^N = \sqrt{\frac{2}{N}}\left(\sin\frac{2\pi j}{N}\right)_{j=1}^N .$$

§ E-mail address: p.repetowicz@physik.tu-chemnitz.de

0305-4470/98/326873+14$19.50

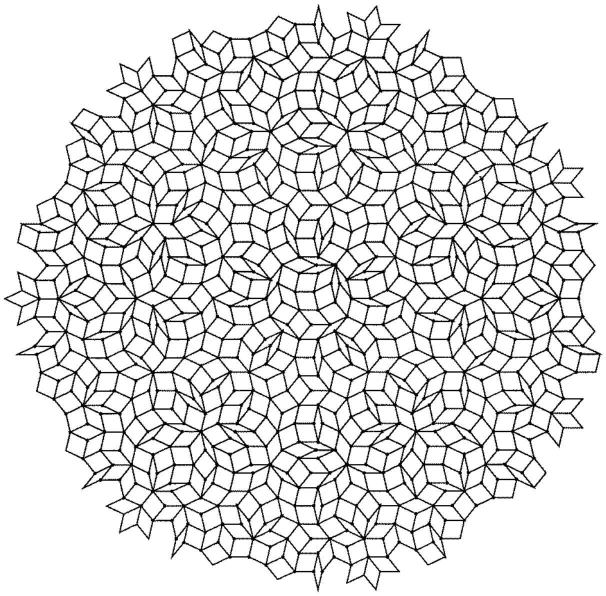

Figure 1. A seven-fold quasilattice.

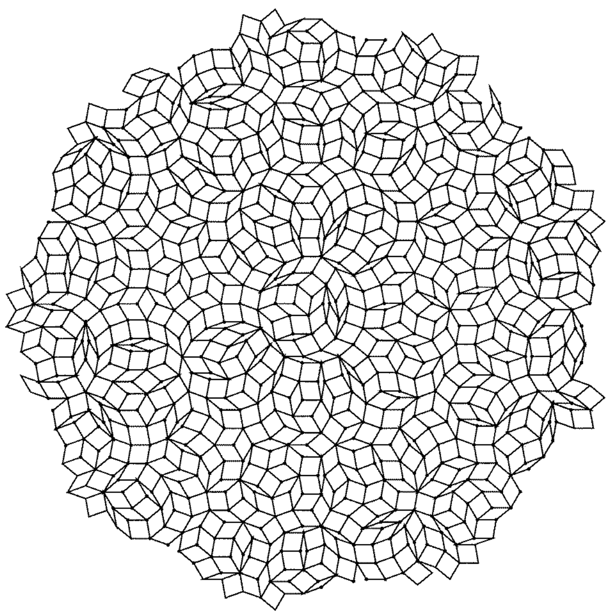

Figure 2. A nine-fold quasilattice.

The $(N-2)$-dimensional perpendicular space $E^{\perp}$ falls in this case into a direct sum of $\frac{N-3}{2}$ planes $E_1, E_2, \ldots, E_{\frac{N-3}{2}}$ and a straight line d which are also invariant by application of the mapping g. The base vectors of the consecutive subspaces take the form:

$$E_1: \qquad \sqrt{\tfrac{2}{N}}\left(\cos\tfrac{2\cdot 2\pi j}{N}\right)_{j=1}^{N} \quad \sqrt{\tfrac{2}{N}}\left(\sin\tfrac{2\cdot 2\pi j}{N}\right)_{j=1}^{N}$$

$$\begin{aligned}
&E_2: \quad \sqrt{\tfrac{2}{N}}\left(\cos\tfrac{2\cdot 3\pi j}{N}\right)_{j=1}^{N} \quad \sqrt{\tfrac{2}{N}}\left(\sin\tfrac{2\cdot 3\pi j}{N}\right)_{j=1}^{N}\\
&\qquad\vdots\\
&E_{\frac{N-3}{2}}: \quad \sqrt{\tfrac{2}{N}}\left(\cos\tfrac{(N-1)\pi j}{N}\right)_{j=1}^{N} \quad \sqrt{\tfrac{2}{N}}\left(\sin\tfrac{(N-1)\pi j}{N}\right)_{j=1}^{N}\\
&d: \quad \sqrt{\frac{1}{N}}(\underbrace{1,\ldots,1}_{N\ \text{times}}).
\end{aligned} \tag{1}$$

According to the general formalism of diffraction pattern calculations (see [1, 7]) of quasilattices obtained by the cut-and-project method, the structure factor reads:

$$F(\boldsymbol{k}_\parallel) = \sum_{\boldsymbol{k}=\boldsymbol{k}_\parallel+\boldsymbol{k}_\perp} \int_W \mathrm{d}^{N-2}r_\perp \, \exp\{\mathrm{i}\boldsymbol{k}_\perp \cdot \boldsymbol{r}_\perp\} \tag{2}$$

where W is a projection of the strip onto $E^\perp$, and $\boldsymbol{k}_\parallel$ and $\boldsymbol{k}_\perp$ are projections of a wavevector $\boldsymbol{k} = 2\pi(h_1,\ldots,h_N)$ from the N-dimensional reciprocal space down to E and the $(N-2)$-dimensional perpendicular space $E^\perp$, respectively. The sum runs over all $\boldsymbol{k}_\perp$'s being assigned to $\boldsymbol{k}_\parallel$ in such a way that $\boldsymbol{k} = \boldsymbol{k}_\parallel + \boldsymbol{k}_\perp$.

The presence of this sum in front of the integral will cause a reduction of the dimension of the solid W. It is known that the minimal dimension of the hyperspace, needed to obtain a N-fold quasilattice by the cut-and-project method, amounts $\phi(N)$ [3, 2] where ϕ is the Eulers totient function. The minimal dimension is also equal to the rank of the diffraction pattern, i.e. to the minimum set of axis vectors which index the diffraction pattern of the structure [4–6]. Because the dimension of E equals two, one expects, that one has indeed to integrate over $(\phi(N)-2)$-dimensional solids. Let us try to substantiate this statement.

In the case of the quasilattices which we examine there is no one-to-one correspondence among $\boldsymbol{k}_\parallel$ and $\boldsymbol{k}_\perp$. It is due to the fact that the perpendicular space $E^\perp$ intersects $\mathbb{Z}^N$. The dimension of this intersection is equal to the 'surplus of dimensions' $p = N - \phi(N)$. Let us assume that $E^\perp \cap \mathbb{Z}^N$ is spanned by a set of vectors $\{\boldsymbol{a}_j\}_{j=1}^{p}$. Let us now take an arbitrary $\boldsymbol{k}_\perp$ and add a vector $2\pi\boldsymbol{V}$, where $\boldsymbol{V} = n_1\boldsymbol{a}_1 + \cdots + n_p\boldsymbol{a}_p \in E^\perp \cap \mathbb{Z}^N$, to it. This addition leads obviously to another, different, $\boldsymbol{k}'_\perp = \boldsymbol{k}_\perp + 2\pi\boldsymbol{V}$, which is, however, assigned to the same $\boldsymbol{k}_\parallel$, because the projection of $2\pi\boldsymbol{V}$ onto E equals zero.

After replacing $\boldsymbol{k}_\perp$ by $\boldsymbol{k}'_\perp$ in formula (2) we obtain:

$$\begin{aligned}
F(\boldsymbol{k}_\parallel) &= \int_W \mathrm{d}^{N-2}r_\perp \, \exp\{\mathrm{i}\boldsymbol{k}_\perp \cdot \boldsymbol{r}_\perp\} \sum_{n_1,\ldots,n_p=-\infty}^{+\infty} \exp\{\mathrm{i}2\pi n_1 \boldsymbol{a}_1 \boldsymbol{r}_\perp\} \cdot \ldots \cdot \exp\{\mathrm{i}2\pi n_p \boldsymbol{a}_p \boldsymbol{r}_\perp\}\\
&= \int_W \mathrm{d}^{N-2}r_\perp \, \exp\{\mathrm{i}\boldsymbol{k}_\perp \cdot \boldsymbol{r}_\perp\} \sum_{h_1,\ldots,h_p=-\infty}^{+\infty} \delta(\boldsymbol{a}_1\boldsymbol{r}_\perp - h_1) \cdot \ldots \cdot \delta(\boldsymbol{a}_p\boldsymbol{r}_\perp - h_p)
\end{aligned} \tag{3}$$

where we applied the following relation $\sum_{n=-\infty}^{+\infty} \exp\{\mathrm{i}2\pi rn\} = \sum_{h=-\infty}^{+\infty} \delta(r-h)$. The product of $p = N - \phi(N)$ delta functions occurring in (3) will diminish the dimension of the solids, over which we have to integrate, from $(N-2)$ to $(N-2-p) = (\phi(N)-2)$ as expected.

Let us now apply these considerations to the cases $N = 7$ and $N = 9$.

First of all we have to determine the intersection $E^\perp \cap \mathbb{Z}^N$. After some lengthy, but straightforward calculations we obtain the following result:

$$E^\perp \cap \mathbb{Z}^N = \begin{cases} (n_3, n_3, n_3, n_3, n_3, n_3, n_3) & \text{for } N = 7, \text{ where } n_3 \in \mathbb{Z} \\ (n_1, n_2, n_3, n_1, n_2, n_3, n_1, n_2, n_3) & \text{for } N = 9, \text{ where } n_1, n_2, n_3 \in \mathbb{Z}. \end{cases} \tag{4}$$

Actually, if we decompose the above vectors to the base vectors of E and $E^{\perp}$ the components parallel to E vanish

$$(n_1, n_2, n_3, n_1, n_2, n_3, n_1, n_2, n_3) = \frac{-n_1 - n_2 + 2n_3}{3}\boldsymbol{v}_2 + \frac{\sqrt{3}}{3}(n_1 - n_2)\boldsymbol{w}_2 + \frac{n_1 + n_2 + n_3}{3}\boldsymbol{d}$$

where $\boldsymbol{v}_2, \boldsymbol{w}_2$ are base vectors of E_2 and read:

$$\boldsymbol{v}_2 = (v_{2j})_{j=1}^{N} := \left(\cos\left(\frac{6\pi}{9} j\right)\right)_{j=1}^{N} \qquad \boldsymbol{w}_2 = (w_{2j})_{j=1}^{N} := \left(\sin\left(\frac{6\pi}{9} j\right)\right)_{j=1}^{N}$$

and

$$\boldsymbol{d} = (\underbrace{1, \ldots, 1}_{N \text{ times}}).$$

Therefore a transformation

$$\boldsymbol{k}_{\text{new}} := \begin{cases} \boldsymbol{k} + 2\pi(n_3, n_3, n_3, n_3, n_3, n_3, n_3) & \text{for } N = 7 \\ \boldsymbol{k} + 2\pi(n_1, n_2, n_3, n_1, n_2, n_3, n_1, n_2, n_3) & \text{for } N = 9 \end{cases}$$

changes $\boldsymbol{k}_{\perp}$ but has no influence on $\boldsymbol{k}_{\parallel}$. Projecting $\boldsymbol{k}$ onto the appropriate spaces E and $E^{\perp}$ and denoting the appropriate projections as π and $\pi^{\perp}$ yields:

$$\boldsymbol{k}_{\parallel\text{new}} = \pi\boldsymbol{k} = \boldsymbol{k}_{\parallel}$$

because $\boldsymbol{v}_2, \boldsymbol{w}_2$ and $\boldsymbol{d}$ are perpendicular to E, and

$$\boldsymbol{k}_{\perp\text{new}} = \pi^{\perp}\boldsymbol{k} = \begin{cases} \boldsymbol{k}_{\perp} + 2\pi(0, 0, 0, 0, n_3) & \text{for } N = 7 \\ \boldsymbol{k}_{\perp} + \dfrac{2\pi}{3}(0, 0, -n_1 - n_2 + 2n_3, \sqrt{3}(n_1 - n_2), 0, 0, n_1 + n_2 + n_3) \\ \qquad \text{for } N = 9. \end{cases}$$

Taking advantage of the above, on the basis of formula (3), we obtain expressions for the structure factor.

For $N = 7$ and $\boldsymbol{r}_{\perp} := (r_{\perp j})_{j=1}^{5}$ we obtain:

$$F(\boldsymbol{k}_{\parallel}) = \int_W \mathrm{d}^{N-2} r_{\perp}\ \exp\{\mathrm{i}\boldsymbol{k}_{\perp} \cdot \boldsymbol{r}_{\perp}\} \sum_{h_3} \delta(h_3 - r_{\perp 5}). \tag{5}$$

For $N = 9$ and $\boldsymbol{r}_{\perp} := (r_{\perp j})_{j=1}^{7}$ one finds:

$$F(\boldsymbol{k}_{\parallel}) = 9\int_W \mathrm{d}^{N-2} r_{\perp} \exp\{\mathrm{i}\boldsymbol{k}_{\perp} \cdot \boldsymbol{r}_{\perp}\} \sum_{h_1, h_2, h_3} \delta(3h_1 - (-r_{\perp 3} + \sqrt{3} r_{\perp 4} + r_{\perp 7})) \cdot \delta(3h_2 - (-r_{\perp 3} - \sqrt{3} r_{\perp 4} + r_{\perp 7})) \cdot \delta(3h_3 - (2r_{\perp 3} + r_{\perp 7})). \tag{6}$$

Ultimately the above formulae take the following form.

For $N = 7$

$$F(\boldsymbol{k}_{\parallel}) = \sum_{h_3} \int_{P_{h_3}} \mathrm{d}\boldsymbol{r}_{\perp}^{(1)}\, \mathrm{d}\boldsymbol{r}_{\perp}^{(3)}\ \exp \mathrm{i}\{\boldsymbol{k}_{\perp}^{(1)} \cdot \boldsymbol{r}_{\perp}^{(1)} + \boldsymbol{k}_{\perp}^{(2)} \cdot \boldsymbol{r}_{\perp}^{(2)}\} \cdot \exp \mathrm{i}\{k_5 h_3\} \tag{7}$$

and for $N = 9$

$$F(\boldsymbol{k}_\parallel) = \sum_{h_1,h_2,h_3} \int_{P_{h_1,h_2,h_3}} \mathrm{d}\boldsymbol{r}_\perp^{(1)}\, \mathrm{d}\boldsymbol{r}_\perp^{(3)}\, \exp \mathrm{i}\{\boldsymbol{k}_\perp^{(1)} \cdot \boldsymbol{r}_\perp^{(1)} + \boldsymbol{k}_\perp^{(3)} \cdot \boldsymbol{r}_\perp^{(3)}\}$$
$$\times \exp \mathrm{i} \left\{ \boldsymbol{k}_\perp^{(2)} \cdot \left(\frac{-h_1 - h_2 + 2h_3}{2}, \frac{\sqrt{3}}{2}(h_1 - h_2) \right) \right\} \cdot \exp \mathrm{i}\{k_7(h_1 + h_2 + h_3)\} \tag{8}$$

where we decomposed the $(N-2)$-dimensional $\boldsymbol{k}_\perp$ and $\boldsymbol{r}_\perp$ vectors to their components in the consecutive invariant subspaces $E_1, \ldots, E_3$ and d:

$$\boldsymbol{k}_\perp := \begin{cases} (\boldsymbol{k}_\perp^{(1)}, \boldsymbol{k}_\perp^{(2)}, k_5) & \text{for } N = 7 \\ (\boldsymbol{k}_\perp^{(1)}, \boldsymbol{k}_\perp^{(2)}, \boldsymbol{k}_\perp^{(3)}, k_7) & \text{for } N = 9 \end{cases} \qquad \text{and analogically for } \boldsymbol{r}_\perp.$$

On the basis of (5) and (6) the solids P_{h_1,h_2,h_3} and P_{h_3} occurring in the integration limits are determined as intersections of the window W with certain hyperplanes:

$$P_{h_3} := W \cap \{r_5 = h_3\}$$
$$P_{h_1,h_2,h_3} := W \cap \left\{ (r_3, r_4, r_7) = \left(\sum_{l=1}^{3} h_l \cos\frac{2\pi}{3} l, \sum_{l=1}^{3} h_l \sin\frac{2\pi}{3} l, \sum_{l=1}^{3} h_l \right) \right\}.$$

They are complicated four-dimensional polytopes and can be described as unions of linear combinations of certain four-dimensional vectors with some additional constraints imposed on the coefficients

$$P_{h_3} := \left\{ \sum_{j=1}^{7} \xi_j \left(\cos\left(\frac{4\pi}{7} j\right), \sin\left(\frac{4\pi}{7} j\right), \cos\left(\frac{6\pi}{7} j\right), \sin\left(\frac{6\pi}{7} j\right) \right) \right.$$
$$\left. \middle| \sum_{j=1}^{7} \xi_j = h_3 \text{ and } \xi_j \in [0, 1] \right\} \tag{9}$$

$$P_{h_1,h_2,h_3} := \left\{ \sum_{j=1}^{9} \xi_j \left(\cos\left(\frac{4\pi}{9} j\right), \sin\left(\frac{4\pi}{9} j\right), \cos\left(\frac{8\pi}{9} j\right), \sin\left(\frac{8\pi}{9} j\right) \right) \middle| \sum_{j=0}^{2} \xi_{3j+p} = h_p \right.$$
$$\left. \text{where } p = 1, \ldots, 3 \text{ and } \xi_j \in [0, 1] \right\}. \tag{10}$$

An essential difficulty which we encounter now is the necessity of integration over fairly complicated four-dimensional polytopes. This can, however, be done by decomposing P_{h_3} and P_{h_1,h_2,h_3} into a union of simpler solids, so-called *simplices*

$$S_h^{(j)} := S_h(\boldsymbol{w}_1^j, \ldots, \boldsymbol{w}_4^j) := \left\{ \sum_{k=1}^{4} \xi_k \boldsymbol{w}_k^j \middle| \sum_{k=1}^{4} \xi_k \leqslant 1,\ \xi_k \in (0, 1) \right\}$$

having disjoint interiors.

The decompositions read:

$$P_{h_3} = \bigcup_{j=1}^{t[h_3]} S_{h_3}^{(j)} \qquad P_{h_1,h_2,h_3} = \bigcup_{j=1}^{t[h_1,h_2,h_3]} S_{h_1,h_2,h_3}^{(j)} \tag{11}$$

where $t[h_3]$ and $t[h_1, h_2, h_3]$ stand for the number of simplices and

$$\mathrm{Int}\,(S_{h_3}^j \cap S_{h_3}^l) = \mathrm{Int}\,(S_{h_1,h_2,h_3}^j \cap S_{h_1,h_2,h_3}^l) = \{\emptyset\} \qquad \text{for } l \neq j.$$

The integrals over simplices $S(\boldsymbol{w}_1, \ldots, \boldsymbol{w}_4)$ can be easily calculated analytically by performing the following variable substitution $\boldsymbol{r} := \sum_{j=1}^{4} \xi_j \boldsymbol{w}_j$:

$$\int_{S(\boldsymbol{w}_1,\ldots,\boldsymbol{w}_4)} \mathrm{d}^4 r \mathrm{e}^{\mathrm{i}\boldsymbol{k}\boldsymbol{r}} = D \int_0^1 \mathrm{d}\xi_1 \int_0^{1-\xi_1} \mathrm{d}\xi_2 \int_0^{1-\xi_1-\xi_2} \mathrm{d}\xi_3 \int_0^{1-\xi_1-\xi_2-\xi_3} \mathrm{d}\xi_4$$
$$\times \exp\left\{\mathrm{i} \sum_{j=1}^{4} \xi_j (\boldsymbol{k} \circ \boldsymbol{w}_j)\right\} = \frac{D}{\mathrm{i}(A_1 - A_2)}$$
$$\times \left[\frac{1}{(A_1 - A_3)} \left(\frac{f(A_1) - f(A_4)}{A_1 - A_4} - \frac{f(A_3) - f(A_4)}{A_3 - A_4}\right)\right.$$
$$\left. - \frac{1}{(A_2 - A_3)} \left(\frac{f(A_2) - f(A_4)}{A_2 - A_4} - \frac{f(A_3) - f(A_4)}{A_3 - A_4}\right)\right]$$
$$\text{where } D = \det[\boldsymbol{w}_1, \boldsymbol{w}_2, \boldsymbol{w}_3, \boldsymbol{w}_4],\ A_j := \boldsymbol{k}\boldsymbol{w}_j \text{ and } f(x) = \mathrm{e}^{-\mathrm{i}\frac{x}{2}} \frac{\sin\frac{x}{2}}{\frac{x}{2}}. \qquad (12)$$

Using formulae (8), (7) and (12), we are able to calculate the structure factor analytically, provided we know the *simplicial decompositions* of the polytopes P_{h_3} and P_{h_1,h_2,h_3}. In other words, the problem we face, is based on the following two steps.

(1) Expressing the polytopes P_{h_3} and P_{h_1,h_2,h_3} as *convex hulls* of certain sets of vectors. For each of the considered polytopes we are looking for four-dimensional vectors $\boldsymbol{w}_1, \ldots, \boldsymbol{w}_m$ such that the smallest convex set comprising them equals to the appropriate polytope:

$$P_{h_3} = \left\{ \sum_{j=1}^{m} \xi_j \boldsymbol{w}_j \,\middle|\, \sum_{j=1}^{m} \xi_j = 1 \text{ and } \xi_j \geqslant 0 \right\} \qquad \text{and accordingly for } P_{h_1,h_2,h_3}.$$

(2) Finding the simplicial decompositions (11) of P_{h_3} and P_{h_1,h_2,h_3}, it means decompositions into simplices with disjoint interiors.

The first step is presented in the appendix. Different algorithms for simplicial decompositions of convex polytopes or equivalently finding all facets of a convex polytope can be taken from [8]. We have, however, devised an algorithm ourselves, treating this case as an interesting problem of linear programming.

3. Comparison with numerical calculations in physical space

A final verification of the correctness of our considerations is a comparison with the structure factor calculated directly from its definition $F(\boldsymbol{k}) := \sum_{\boldsymbol{r}} \exp\{\mathrm{i}\boldsymbol{k} \cdot \boldsymbol{r}\}$. For this purpose, one has to generate a sufficiently big cluster of atoms so that the results of the numerical calculations depend on neither the size nor the shape of the cluster. One achieves that by taking the number of atoms of the order of 2000 and 5000 for the seven- and nine-fold quasilattices, respectively. In figures 3 and 4 one can see cross sections of the diffraction pattern of seven-fold quasilattices along the Y- and X-axes, respectively. The solid line represents the numerical calculations, whereas the analytical results obtained from formulae (8), (7) and (12) are marked with dots. There is a perfect coincidence both for the positions of peaks and their intensities. The full two-dimensional diffraction pattern exhibiting a marvellous 14-fold symmetry has been presented in figure 5. In a similar way we have presented the diffraction pattern of the nine-fold quasilattice. Figures 6 and 7 show cross sections of the diffraction pattern along the Y- and X-axes, respectively. The full two-dimensional diffraction pattern has been presented in figure 8. As far as the positions of

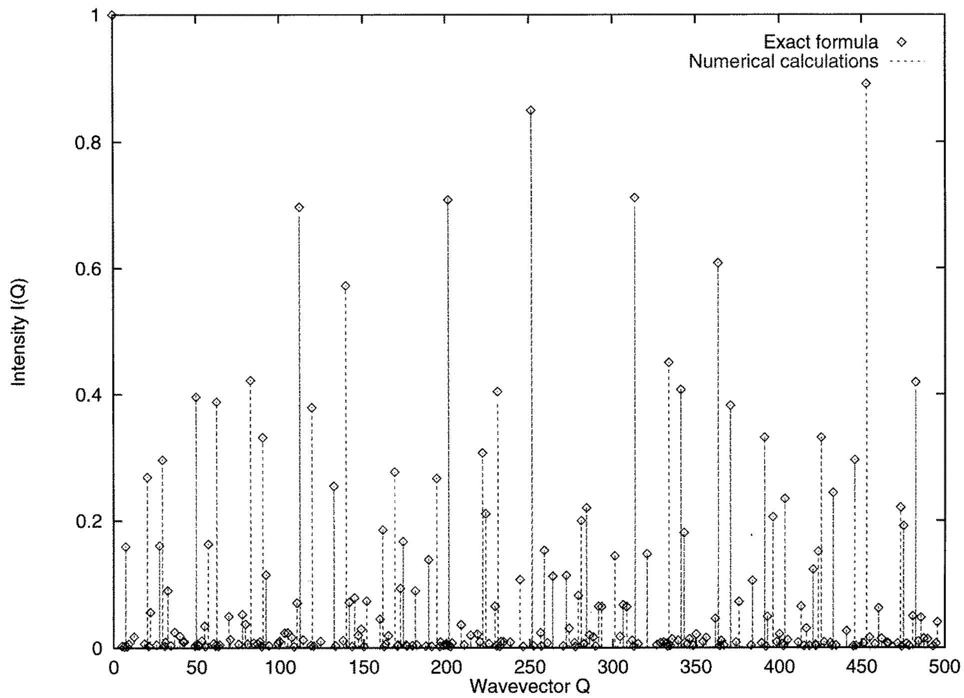

Figure 3. Diffraction pattern along the Y-axis for the seven-fold quasilattice.

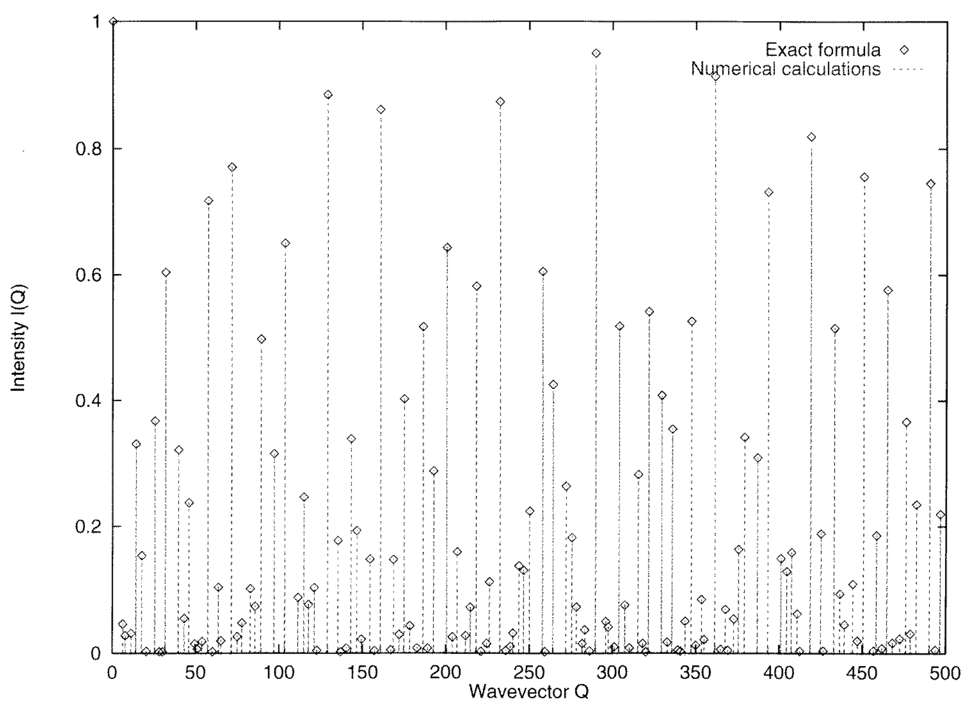

Figure 4. Diffraction pattern along the X-axis for the seven-fold quasilattice.

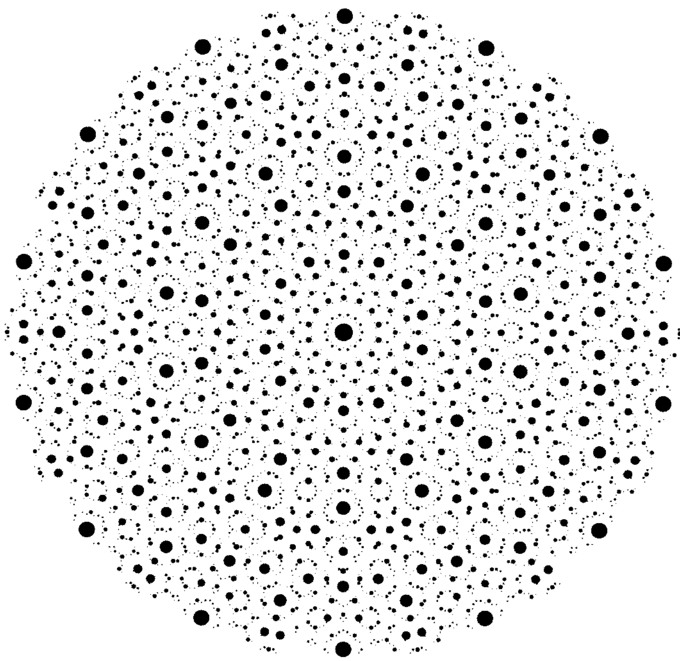

Figure 5. Diffraction pattern of the seven-fold quasilattice.

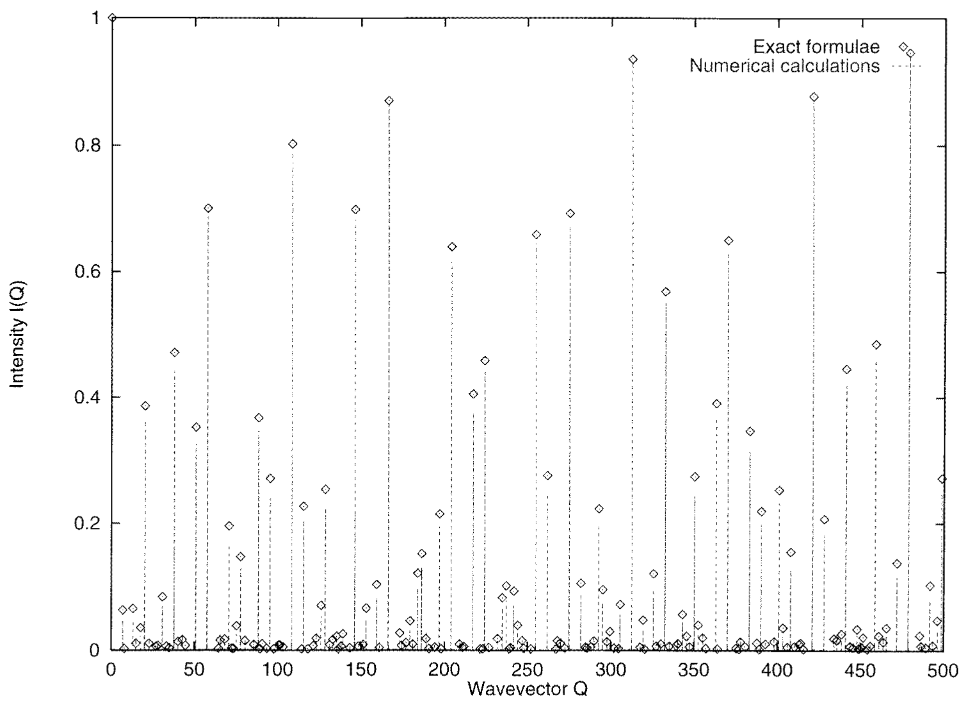

Figure 6. Diffraction pattern along the Y-axis for the nine-fold quasilattice.

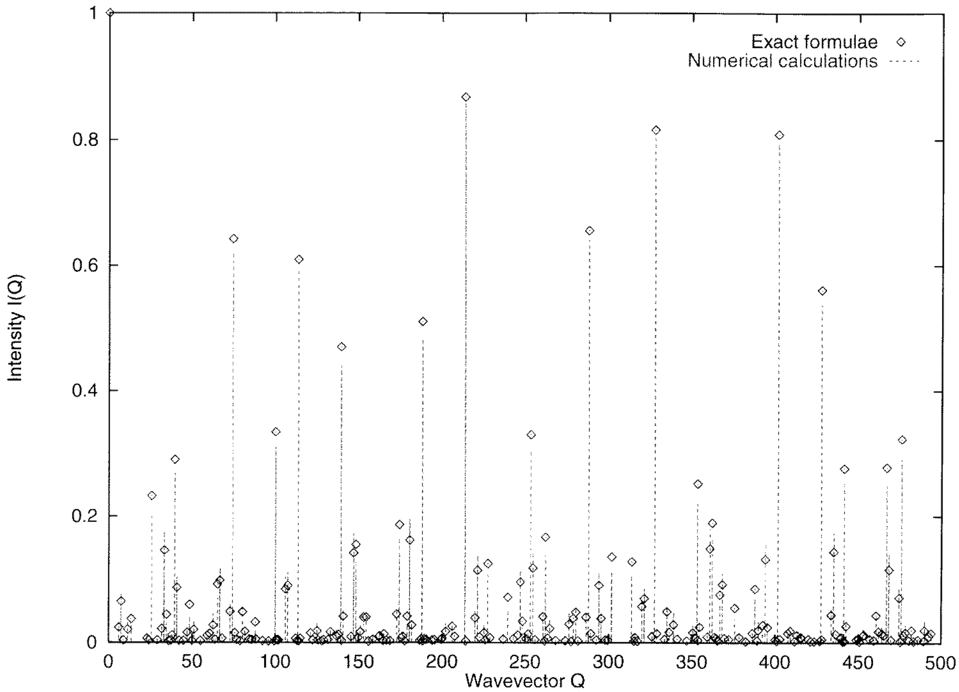

Figure 7. Diffraction pattern along the X-axis for the nine-fold quasilattice.

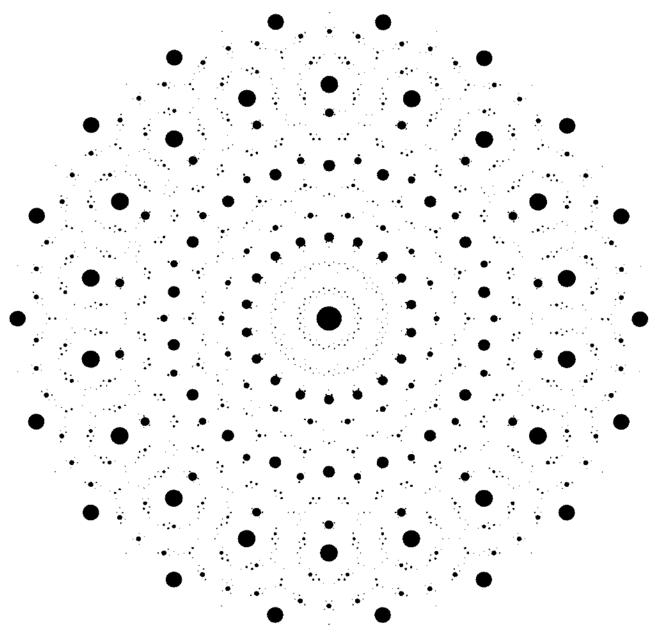

Figure 8. Diffraction pattern of the nine-fold quasilattice.

peaks are concerned, there is an agreement among the analytical results and the numerical calculations. There are, however, some deviations in the amplitudes of certain peaks.

These discrepancies decrease systematically with the number of sites of the cluster used to numerical calculations. It seems that the convergence of the Fourier transforms of a finite cluster is much slower then in the case of the seven fold quasilattice. This may be due to the fact that the number of integrals in the formulae for the structure factor (8), (7), or equivalently the number of different polytopes, over which one has to integrate, is greater than in the former case of the seven-fold quasilattice. It is worth remarking that we achieve a faster convergence of the numerically calculated structure factor for symmetric, round shape clusters as shown in figures 1 and 2.

4. Conclusions

The calculated diffraction patterns exhibit the following properties.

(1) They have a $2N$-fold symmetry which is a consequence of the N-fold symmetry of the quasilattice and an invariance of the diffraction pattern with respect to inversion.

(2) They have certain scaling features, following from the invariance of the quasilattices under inflation, see [2].

(3) The diffraction spots, that is all $\boldsymbol{k}$ assigned to non-vanishing peaks, fill the plane densely.

In this paper we have investigated in details the cases of seven- and nine-fold quasilattices. The choice of right these values of N was mostly due to the fact that in both cases the polytopes in the perpendicular space are four-dimensional and thereby the formalism of calculations is similar. It is, however, worth to emphasize that the consideration of the generic case, where N is an arbitrary integer, does not present substantial difficulties.

Acknowledgments

We would like to express our sincere thanks to Dr Uwe Grimm and P Bieniarz for the attentive reading of the manuscript and for valuable comments and discussion. I also thank the referee for the critical opinions which considerably improved the scientific value of this work.

Appendix. Presenting the four-dimensional polytopes P_{h_3} and P_{h_1,h_2,h_3} as convex hulls of certain sets of vectors

Let us note that both kinds of polytopes P_{h_3} and P_{h_1,h_2,h_3} can be presented as a projection of a certain N-dimensional solid down to the perpendicular space $E^{\perp}$.

A.1. The case $N = 9$

Let us focus on P_{h_1,h_2,h_3} and define a following multitude of points embedded in the nine-dimensional space:

$$S_{h_1,h_2,h_3} := \left\{ (\xi_1, \ldots, \xi_9) \middle| \sum_{j=0}^{2} \xi_{3j+p} = h_p,\ p = 1, \ldots, 3 \text{ and } \xi_j \in [0, 1] \right\}. \tag{13}$$

The above solid, which is actually an intersection of the unit hypercube with a hyperplane given by the right-hand side equations in (13), yields our four-dimensional polytope P_{h_1,h_2,h_3}

when projecting onto $E_1 \oplus E_3$ (cf (10)). The perpendicular space $E^\perp$ has the following decomposition $E^\perp = E_1 \oplus E_2 \oplus E_3 \oplus d$ (see (1)).

$$P_{h_1,h_2,h_3} = \pi^\perp S_{h_1,h_2,h_3}$$

where $\pi^\perp$ is a projection onto $E_1 \oplus E_3$.

P_{h_1,h_2,h_3} is a convex hull of the projections of all vertices of the underlying nine-dimensional solid S_{h_1,h_2,h_3}.

The only point which remained now is to find the vertices of the solid S_{h_1,h_2,h_3}. Taking an attentive look at definition (13) leads to a conclusion that the solid S_{h_1,h_2,h_3} can be treated as a Cartesian product of three three-dimensional solids:

$$S_{h_1,h_2,h_3} = S^{(1)}_{h_1} \otimes S^{(2)}_{h_2} \otimes S^{(3)}_{h_3}$$

$$\text{where } S^{(j)}_h := \left\{ \left(\sum_{p=0}^{2} \xi_{3\cdot p+j} \boldsymbol{e}_{3\cdot p+j} \right) \middle| \sum_{p=0}^{2} \xi_{3\cdot p+j} = h, \xi_j \in [0,1] \right\} \tag{14}$$

where $\boldsymbol{e}_j$ is a unit vector from the canonical base in nine-dimensional space.

Therefore the sought after vertices of S_{h_1,h_2,h_3} can be obtained as all possible sums of vertices of the consecutive solids $S^{(1)}_{h_1}$, $S^{(2)}_{h_2}$, $S^{(3)}_{h_3}$. In other words, they take the form:

$$\boldsymbol{w}^{(1)}_j + \boldsymbol{w}^{(2)}_p + \boldsymbol{w}^{(3)}_r \qquad \text{where } \boldsymbol{w}^{(l)}_j \text{ are vertices of } S^{(l)}. \tag{15}$$

On the other hand, we can easily find the vertices of $S^{(j)}_h$, they read:

$$\text{vertices of } S^{(j)}_h = \begin{cases} \boldsymbol{e}_{3\cdot 0+j}, \boldsymbol{e}_{3\cdot 1+j}, \boldsymbol{e}_{3\cdot 2+j} & \text{if } h = 1 \text{ (equilateral triangle)} \\ -\boldsymbol{e}_{3\cdot 0+j}, -\boldsymbol{e}_{3\cdot 1+j}, -\boldsymbol{e}_{3\cdot 2+j} & \text{if } h = 2 \text{ (inverted triangle)} \\ \boldsymbol{0} & \text{if } h = 0 \text{ or } h = 3 \text{ (a point).} \end{cases} \tag{16}$$

Actually the vertices of $S^{(j)}_2$ differ from formula (16) and read

$$\boldsymbol{e}_{3\cdot 0+j} + \boldsymbol{e}_{3\cdot 1+j}, \boldsymbol{e}_{3\cdot 1+j} + \boldsymbol{e}_{3\cdot 2+j}, \boldsymbol{e}_{3\cdot 2+j} + \boldsymbol{e}_{3\cdot 0+j}$$

but after projecting down to $E^\perp$ we get the same vectors in both cases.

Making use of both above formulae (15) and (16) and taking into account that the indices h_1, h_2, h_3 can only accept integer values ranging from 0 to 3 we have enumerated all possible, different polytopes S_{h_1,h_2,h_3} and their vertices in table A1. Two polytopes are considered to be different if they cannot be transformed into each other through an inversion or an orthogonal transformation. The manner in which the polytopes change after applying certain transformations is expressed in the following lemma.

Lemma. Let II be an inversion and g an orthogonal transformation defined as follows

$$g = \begin{pmatrix} \cos(\frac{4\pi}{9}) & \sin(\frac{4\pi}{9}) & 0 & 0 \\ -\sin(\frac{4\pi}{9}) & \cos(\frac{4\pi}{9}) & 0 & 0 \\ 0 & 0 & \cos(\frac{8\pi}{9}) & \sin(\frac{8\pi}{9}) \\ 0 & 0 & -\sin(\frac{8\pi}{9}) & \cos(\frac{8\pi}{9}) \end{pmatrix}.$$

Then following equalities hold:

$$II P_{h_1,h_2,h_3} = P_{3-h_1,3-h_2,3-h_3} \qquad \text{and} \qquad g P_{h_1,h_2,h_3} = P_{h_2,h_3,h_1}.$$

In other words an application of the ‘rotation’ g is due to a transition to another polytope with cyclic permuted indices.

Table A1. A list of all possible different solids S_{h_1,h_2,h_3}. $\boldsymbol{e}_j$ is a unit vector from the canonical base.

h_1	h_2	h_3	Vertices of S_{h_1,h_2,h_3}	Number of vertices	$h_1+h_2+h_3$	Remarks
1	0	0	$\boldsymbol{e}_{3\cdot p+1}$	3	1	
0	1	0	$\boldsymbol{e}_{3\cdot p+2}$	3	1	border set
0	0	1	$\boldsymbol{e}_{3\cdot p+3}$	3	1	
1	1	0	$\boldsymbol{e}_{3\cdot p+1}+\boldsymbol{e}_{3\cdot q+2}$	9	2	
0	1	1	$\boldsymbol{e}_{3\cdot p+2}+\boldsymbol{e}_{3\cdot q+3}$	9	2	
1	0	1	$\boldsymbol{e}_{3\cdot p+3}+\boldsymbol{e}_{3\cdot q+1}$	9	2	
2	0	0	$-\boldsymbol{e}_{3\cdot p+1}$	3	2	
0	2	0	$-\boldsymbol{e}_{3\cdot p+2}$	3	2	border set
0	0	2	$-\boldsymbol{e}_{3\cdot p+3}$	3	2	
1	1	1	$\boldsymbol{e}_{3\cdot p+1}+\boldsymbol{e}_{3\cdot q+2}+\boldsymbol{e}_{3\cdot r+3}$	27	3	
2	1	0	$-\boldsymbol{e}_{3\cdot p+1}+\boldsymbol{e}_{3\cdot q+2}$	9	3	
0	2	1	$-\boldsymbol{e}_{3\cdot p+2}+\boldsymbol{e}_{3\cdot q+3}$	9	3	
1	0	2	$-\boldsymbol{e}_{3\cdot p+3}+\boldsymbol{e}_{3\cdot q+1}$	9	3	
2	0	1	$-\boldsymbol{e}_{3\cdot p+1}+\boldsymbol{e}_{3\cdot q+3}$	9	3	
1	2	0	$-\boldsymbol{e}_{3\cdot p+2}+\boldsymbol{e}_{3\cdot q+1}$	9	3	
0	1	2	$-\boldsymbol{e}_{3\cdot p+3}+\boldsymbol{e}_{3\cdot q+2}$	9	3	
2	1	1	$-\boldsymbol{e}_{3\cdot p+1}+\boldsymbol{e}_{3\cdot q+2}+\boldsymbol{e}_{3\cdot r+3}$	27	4	
1	2	1	$-\boldsymbol{e}_{3\cdot p+2}+\boldsymbol{e}_{3\cdot q+3}+\boldsymbol{e}_{3\cdot r+1}$	27	4	
1	1	2	$-\boldsymbol{e}_{3\cdot p+3}+\boldsymbol{e}_{3\cdot q+1}+\boldsymbol{e}_{3\cdot r+2}$	27	4	
2	2	0	$-\boldsymbol{e}_{3\cdot p+1}-\boldsymbol{e}_{3\cdot q+2}$	9	4	
0	2	2	$-\boldsymbol{e}_{3\cdot p+2}-\boldsymbol{e}_{3\cdot q+3}$	9	4	
2	0	2	$-\boldsymbol{e}_{3\cdot p+3}-\boldsymbol{e}_{3\cdot q+1}$	9	4	
3	1	0	$\boldsymbol{e}_{3\cdot q+2}$	3	4	
0	3	1	$\boldsymbol{e}_{3\cdot q+3}$	3	4	border set
1	0	3	$\boldsymbol{e}_{3\cdot q+1}$	3	4	
3	0	1	$\boldsymbol{e}_{3\cdot q+3}$	3	4	
1	3	0	$\boldsymbol{e}_{3\cdot q+1}$	3	4	border set
0	1	3	$\boldsymbol{e}_{3\cdot q+2}$	3	4	

Proof. It holds per definition $g(\boldsymbol{v}_j)=\boldsymbol{v}_{j-1}$ where $\boldsymbol{v}_j := \left(\cos\left(\frac{4\pi}{9}j\right), \sin\left(\frac{4\pi}{9}j\right), \cos\left(\frac{8\pi}{9}j\right), \sin\left(\frac{8\pi}{9}j\right)\right)$. Thus,

$$\sum_{j=1}^{N}\xi_j g(\boldsymbol{v}_j)=\sum_{j=1}^{N}\xi_{j+1}\boldsymbol{v}_j$$

and under the transformation g the coefficients ξ_j change as follows

$$\xi_j \longrightarrow \eta_j=\xi_{j+1}.$$

Thereafter the index of the 'rotated' polytope reads

$$h'_p = \sum_{j=0}^{2} \eta_{3\cdot j+p} = \sum_{j=0}^{2} \xi_{3\cdot j+p+1} = h_{p+1}.$$

Note that $II(\boldsymbol{v}_j) := -\boldsymbol{v}_j = \sum_{k\neq j} \boldsymbol{v}_k$. It is due to the fact that $\sum_{k=1}^{9} \boldsymbol{v}_k = \vec{0}$. Therefore,

$$\sum_{j=1}^{N} \xi_j II(\boldsymbol{v}_j) = \sum_{j=1}^{N} \xi_j \sum_{k\neq j} \boldsymbol{v}_k = \sum_{k} \boldsymbol{v}_k \sum_{j\neq k} \xi_j.$$

It means that under the inversion II $\xi_j \longrightarrow \eta_j = \sum_{k\neq j} \xi_k$. The remainder of the proof is now straightforward. The index of the 'rotated' polytope reads:

$$h'_p = \sum_{j=0}^{2} \eta_{3\cdot j+p} = \sum_{j=0}^{2} \sum_{k\neq 3\cdot j+p} \xi_k = 3 \cdot \sum_{k=1}^{9} \xi_k - \sum_{j=0}^{2} \xi_{3\cdot j+p} = 3(h_1 + h_2 + h_3) - h_p.$$

Taking the result modulo 3 we obtain $h'_p = 3 - h_p$. □

Note that not all polytopes P_{h_1,h_2,h_3} are relevant for our considerations because some of them are border sets which have zero-volume and therefore the integrals over them in (8) vanish. Altogether, there are six different polytopes, plus their images under the mapping g, which have to be taken into account by our analytical calculations (see table A1).

A.2. The case $N = 7$

The solids P_{h_3} (see definition (9)) are even simpler to investigate than the former case. Reasoning similarly as in section A.1 leads to the following conclusion.

Statement. P_{h_3} is a convex hull of the projections of all vertices of an underlying seven-dimensional solid S_{h_3} which is defined as follows

$$S_{h_3} := \left\{ (\xi_1, \ldots, \xi_7) \middle| \sum_{j=1}^{7} \xi_j = h_3 \text{ and } \xi_j \in [0, 1] \right\}.$$

Table A2. All possible different solids S_{h_3}. $\boldsymbol{e}_j$ is a unit vector from the canonical base.

h_3	Vertices of S_{h_3}	Number of vertices	Remarks
1	$\boldsymbol{e}_i$	7	
2	$\boldsymbol{e}_i + \boldsymbol{e}_{i+1}$ $\boldsymbol{e}_i + \boldsymbol{e}_{i+2}$ $\boldsymbol{e}_i + \boldsymbol{e}_{i+3}$	$3 \cdot 7$	All possible sums of pairs of vectors $\boldsymbol{e}_i + \boldsymbol{e}_j$ $i \neq j$
3	$\boldsymbol{e}_i + \boldsymbol{e}_{i+1} + \boldsymbol{e}_{i+2}$ $\boldsymbol{e}_i + \boldsymbol{e}_{i+2} + \boldsymbol{e}_{i+4}$ $\boldsymbol{e}_i + \boldsymbol{e}_{i+3} + \boldsymbol{e}_{i+6}$ $\boldsymbol{e}_i + \boldsymbol{e}_{i+4} + \boldsymbol{e}_{i+6}$ $\boldsymbol{e}_i + \boldsymbol{e}_{i+1} + \boldsymbol{e}_{i+3}$	$5 \cdot 7$	All possible sums of triples of vectors $\boldsymbol{e}_i + \boldsymbol{e}_j + \boldsymbol{e}_k$ $i \leqslant j \leqslant k$

This solid is indeed an intersection of a seven-dimensional unit hypercube with a hyperplane determined by the equation on the right-hand side of the definition $\sum_{j=1}^{7} \xi_j = h_3$. Due to the fact that the hyperplane is six-dimensional, all vertices of S_{h_3} are obtained as intersections of the hyperplane with all edges of the unit hypercube. There are $7 \cdot 2^6$ edges, each of which can be described as a multitude of points (ξ_j) having the following property. Exactly one component of these points is an independent variable ranging from 0 to 1, whereas the other components can accept exactly two values, either 0 or 1, that is

$$(\xi_j) = (\theta_1, \ldots, \theta_{p-1}, t_p, \theta_{p+1}, \ldots, \theta_7) \qquad \text{where } t_p \in [0, 1], \theta_j \in \{0, 1\}.$$

Inserting the above expression to the definition of the hyperplane yields: $t_p = h_3 - \sum_{k \neq p} \theta_k$. It follows that t_p has to be an integer either 0 or 1, because both h_3 and $\sum_{k \neq p} \theta_k$ are integers and $t_p \in [0, 1]$. Therefore, considering sequentially the cases $h_3 = 1, 2, 3$ we calculated the vertices of the solids S_{h_3} and enumerated them in table A2. It turns out that we can limit ourselves to the cases $h_3 = 1, 2, 3$ because the solids S_{h_3} (and accordingly P_{h_3}) change under inversion in the following fashion: $IIS_{h_3} = S_{7-h_3}$. Because of that the polytopes P_{h_3} for $h_3 = 4, 5, 6$ are inversions of the appropriate P_{7-h_3}.

A.3. General remarks

It is also worth paying attention to another meaning of the information gathered in tables A1 and A2. The volumes of the polytopes P_{h_3} and P_{h_1,h_2,h_3} determine the occurrence frequency of certain vertices in our quasilattice. Let us focus on P_{h_1,h_2,h_3} and denote $n_1, \ldots, n_9$ as indices of a vertex in the nine-fold quasilattice. From the homogeneous distribution of the grid-points in the perpendicular space† and from the definition of the polytopes P_{h_1,h_2,h_3} it follows that the volume of P_{h_1,h_2,h_3} determines the occurrence frequency of vertices for which $h_p = \sum_{j=0}^{2} n_{3\cdot j+p}$.

References

[1] Jaric M V 1986 Diffraction from quasi-crystals: Geometric structure factor *Phys. Rev.* B **34** 7

[2] Niizeki K 1989 Self-similarity of quasilattices in two dimensions: I. The n-gonal quasilattice *J. Phys. A: Math. Gen.* **22** 193–204

[3] Hiller H 1985 *Acta Crystallogr.* A **41** 541

[4] Rokhsar D S *et al* 1988 *Acta Crystallogr.* A **44** 197–211

[5] Janssen T 1988 *Phys. Rep.* **168** 55–113

[6] Steurer W 1990 *Z. Kristalogr.* **190** 179–234

[7] Janssen T 1988 *Phys. Lett.* **2** 55–113

[8] Mattheiss T H and Rubin D 1980 A survey and comparison of methods for finding all vertices of convex polyhedral sets *Math. Oper. Res.* **5** 167–85 selected papers

[9] de Bruijn N G 1981 *Nederl. Akad. Wetensch. Proc. Ser.* A **43** 39–66

[10] Kalugin P A, Kitaev A Yu and Levitov L S 1985 *J. Physique* **46** L601

[11] Kramer P and Neri R 1984 *Acta Crystallogr.* A **40** 580

[12] Duneau M and Katz A 1985 *Phys. Rev. Lett.* **54** 2688

[13] Elser V 1985 *Phys. Rev.* B **32** 4892

† More precisely, the grid-points are distributed with a constant density only inside the polytopes P_{h_1,h_2,h_3}.